Stoch Environ Res Risk Assess (2013) 27:77–89
DOI 10.1007/s00477-012-0555-3

ORIGINAL PAPER

Stochastic control of a micro-dam irrigation scheme for dry season farming

Koichi Unami · Macarius Yangyuoru · Abul Hasan Md. Badiul Alam · Gordana Kranjac-Berisavljevic

Published online: 18 January 2012

Abstract Micro-dams are expected to be feasible options for water resources development in semi-arid regions such as the Guinea savanna agro-ecological zone of West Africa. An optimal water management strategy in a micro-dam irrigation scheme supplying water from an existing reservoir to a potential command area is discussed in this paper based on the framework of stochastic control. Water intake facilities are assumed to consist of photovoltaic pumping system units and hoses. The knowledge of current states of the storage volume of the reservoir and the soil moisture in the command area is fed-back to the intake flow rate. A system of two stochastic differential equations is proposed as a model for the dynamics of the micro-dam irrigation scheme, so that temporally backward solution of the Hamilton–Jacobi–Bellman equation determines an optimal control, which represents the optimal water management strategy. A computational procedure using the finite element method is successfully implemented to provide comprehensive information on the optimal control. The results indicate that the water initially stored in the reservoir can support full irrigation for about 80 days under the optimal water management strategy, which is predominantly based on the demand-side principle. However, the volatility of the soil moisture in the command area must be reasonably small.

Keywords Micro-dam irrigation · Dry season farming · Stochastic control · Hamilton–Jacobi–Bellman equation · Finite element method

K. Unami (✉) · A. H. Md. Badiul Alam
Graduate School of Agriculture, Kyoto University, Sakyo-ku, Kyoto 606-8502, Japan
e-mail: unami@adm.kais.kyoto-u.ac.jp

A. H. Md. Badiul Alam
e-mail: alam@kais.kyoto-u.ac.jp

M. Yangyuoru
Institute of Agricultural Research, University of Ghana, P. O. Box 68, Accra, Ghana
e-mail: macarius_y@yahoo.com

G. Kranjac-Berisavljevic
UDS International, University for Development Studies, P. O. Box TL 1350, Tamale, Ghana
e-mail: novagordanak@gmail.com

1 Introduction

Irrigation in general involves taking water from natural or artificial sources and supplying it to command areas where crops are grown. Different scales and types of irrigation schemes are being practiced throughout the world. In some regions, small reservoirs or tanks are built to provide common artificial water sources for rural communities. Tank irrigation systems in Monsoon Asia have a long history, and discussions on better management of them are still ongoing. Arumugam and Mohan (1997) proposed a supply-side decision support system for the release strategy from Veeranam Lake, which is a large historic irrigation tank in South India with a capacity of 26 million m^3. Unami et al. (2005) investigated the optimal water management strategy for a system of three tanks irrigating paddy fields of 40 ha in Japan. Srivastava et al. (2009) examined a rainwater recycling system consisting of six tanks and five open wells for the full irrigation of the command area of 23 ha in Eastern India. Guerra et al. (1990) analyzed the hydrological processes in terraced rice fields with farm reservoirs extending in central Luzon, Philippines. A farm reservoir of their study with a capacity of 2,000 m^3 can support dry season rice irrigation for an

area of 0.4 ha. Panigrahi et al. (2007) carried out experimental studies on a rainfed rice-mustard cropping system consisting of a small on-farm reservoir with a capacity of 61 m^3 and a farm area of 800 m^2. It was revealed that such a system is an economically feasible option for small-scale supplemental irrigation. Smallholder irrigation schemes are also being developed in semi-arid regions of Sub-Saharan Africa (SSA), where erratic rainfall and high evaporation are serious constraints on agricultural production. Micro-dams, dugouts, sub-surface runoff harvesting tanks, and rooftop rainwater harvesting systems are all different rainwater harvesting practices found in the Makanya catchment of rural Tanzania (Pachpute et al. 2009). Here, the smallholder farmers have locally established robust water allocation arrangements among the micro-dams interconnected with furrows (Mul et al. 2011). Makurira et al. (2007) analyzed the water balance of the Manoo micro-dam system, which is part of the Makanya catchment. The storage capacity of the micro-dams in the Makanya catchment ranges from 200 to 1,600 m^3. Ngigi et al. (2005 found that small on-farm reservoirs with capacities of 30–100 m^3 are adequate for supplemental irrigation to produce cabbage in the Laikipia district of Kenya, when they are combined with plot-scale low-head drip irrigation systems, which were introduced in the late 1990s. However, Kulecho and Weatherhead (2005) observed that the drip irrigation system was often discontinued in different parts of eastern Kenya due to lack of maintenance, irrelevant cultural background, and unreliable water supply. The Guinea savanna agro-ecological zone of West Africa is drawing research attention recently because of the extreme contrast between rainy and dry seasons (ILRI, 1993). Thousands of micro-dams are distributed over the upper and central parts of the Volta Basin (Liebe et al. 2005; Liebe et al. 2009; Leemhuis et al. 2009). The command areas of Tono and Dorongo irrigation schemes in the Upper East Region of Ghana are 2,500 and 10 ha, respectively. Mdemu et al. (2009) noticed that the smaller Dorongo scheme, which alone experienced drought, had better water productivity than that in the larger Tono scheme. Faulkner et al. (2008) made comparison between another set of two small reservoir irrigation schemes, namely, Tanga and Weega schemes in the Upper East Region of Ghana, where water demand in the irrigated crop fields was estimated to be in the range of 3.7–5.9 mm/day on weekly basis. In both schemes, the reservoirs' capacities are almost the same with command areas of 1.6 and 6.0 ha in the Tanga and the Weega schemes, respectively. This variance resulted in different irrigation water depths actually supplied during the experimental period, which were in the ranges of 22.0–37.9 and 8.9–14.4 mm/day in the Tanga and the Weega schemes, respectively. The above two comparative studies of the irrigation schemes in Ghana attributed the reason for better performance of the schemes with scarce water availability to efficient water management, which might reduce some of the water losses as Carter et al. (1999) considered.

From the above-mentioned literature review, it can be inferred that more research effort should be directed toward seeking the maximum performance of the minimum sized irrigation schemes, though the operation of micro-dams is not yet clearly understood in conjunction with small-scale subsistence farming managed at the community level in semi-arid SSA. In this paper, a comprehensive description of an optimal water management strategy for a micro-dam existing in the Northern Region of Ghana, having a capacity of 14,748 m^3 and fully irrigating a potential command area of 840 m^2, is outlined. The large dam capacity relative to the small command area is in fact quite reasonable under the assumption that no inflow to the reservoir can be expected during the whole period of dry season irrigation from mid-November to mid-March, which may be 120 days. The water level of the reservoir monotonically decreases in the dry season, while it is multiply utilized for domestic use, livestock watering, and bricks molding, as commonly practiced in SSA (Senzanje et al. 2008). Importance of the micro-dam as an aquatic habitat is secondary (Unami et al. 2012). Therefore, water management should primarily aim neither to empty the reservoir nor dry up the command area during the irrigation period, regardless of economic performance. A minimum stochastic model is developed to represent the physical processes in the micro-dam irrigation scheme to be optimally managed. The storage volume of the reservoir, the volume of readily available water contained in the soil of the command area, and the intake flow rate from the reservoir for irrigation to the command area are all considered as stochastic processes. A rigorous stochastic control approach that solves the Hamilton–Jacobi–Bellman (HJB) equation is employed. This method has an advantage over the conventional scenario-based optimization with a simulation method that do not take all the events that may occur into account (Srivastava 1996) or with an inexact programming method of predetermining the bounds of uncertainties (Lu et al. 2009).

The analytical or numerical solutions of the HJB equations are being studied mostly in the field of financial engineering where economic indices such as discounted utilities are to be maximized (Morimoto and Kawaguchi 2002; Chaumont et al. 2006; Baten and Miah 2007; Yiu et al. 2010). However, the concept presented here does not explicitly involve the economic aspect of the micro-dam irrigation schemes, but the determination of the optimal water management strategy is mathematically reduced to a stochastic control problem maximizing the expectation of the first exit time from a spatio-temporal domain where the stochastic processes should stay within. A computational

procedure based on the finite element method is implemented to give a comprehensive description of the optimal water management strategy as well as the values of expected first exit time.

In the next Sect. 2, the physical details of the micro-dam irrigation scheme as well as the surrounding environment are described. In Sect. 3, the stochastic model is developed to formulate the stochastic control problem. In Sect. 4, being the main objective of this paper, it is demonstrated that the stochastic control problem can be numerically solved to determine the optimal intake flow rate based on the knowledge of current states of the storage volume of the reservoir and the soil moisture in the command area. Section 5 presents the conclusions.

2 Description of the micro-dam irrigation scheme

Unami et al. (2009) have monitored the hydrology of a Ghanaian inland valley containing six micro-dams (Dam 0 through Dam 5), which collect ephemeral surface flow after torrential rains and seepage flow of subsurface water from the ground during the rainy season ahead of the dry season. Figure 1 is a map showing the positions of the six micro-dams in relief of the inland valley depicted using the SRTM digital elevation data (Farr et al. 2007). Groundwater resources in the inland valley are not reliable, since shallow hand dug wells (HDWs) often dry up and deeper tube wells produce brackish water (Unami et al., 2012). Out of the six micro-dams, the most upstream one (Dam 5), located at coordinates 09°28′15″N 001°03′21″W and having a catchment area of 42 ha, is chosen as the micro-dam irrigating the potential command area during the dry season. In the catchment, seepage flows in the hydromorphic farmlands contribute to runoff significantly (Unami and Alam, in press). Figure 2 shows a satellite image of the micro-dam irrigation scheme, whose frame is delineated in Fig. 1. There is no perennial natural water source in the nearby area, but Dam 5 provides two adjacent communities with year-round water source. Dam 5 is equipped with a concrete spillway of 14.7 m wide and underground pipes connected to HDWs, which are installed out of the frame of Fig. 2. Some shallow tube wells (STWs) have also been constructed in the vicinity of Dam 5. Locations of the two STWs are shown in Fig. 2. Water from the HDWs and the STWs are primarily used for domestic purposes in the communities. The site of Dam 5 is fenced with barbed wire to prevent grazing animals from entering, but this arrangement is not working perfectly due to poor maintenance.

Figure 3 shows the rainfall intensity and water level of Dam 5 observed every 15 min during the period from September 1, 2007 through to March 24, 2011. A drop of the water level occurring every dry season is linear irrespective of the stages, suggesting that evaporation from the water surface is

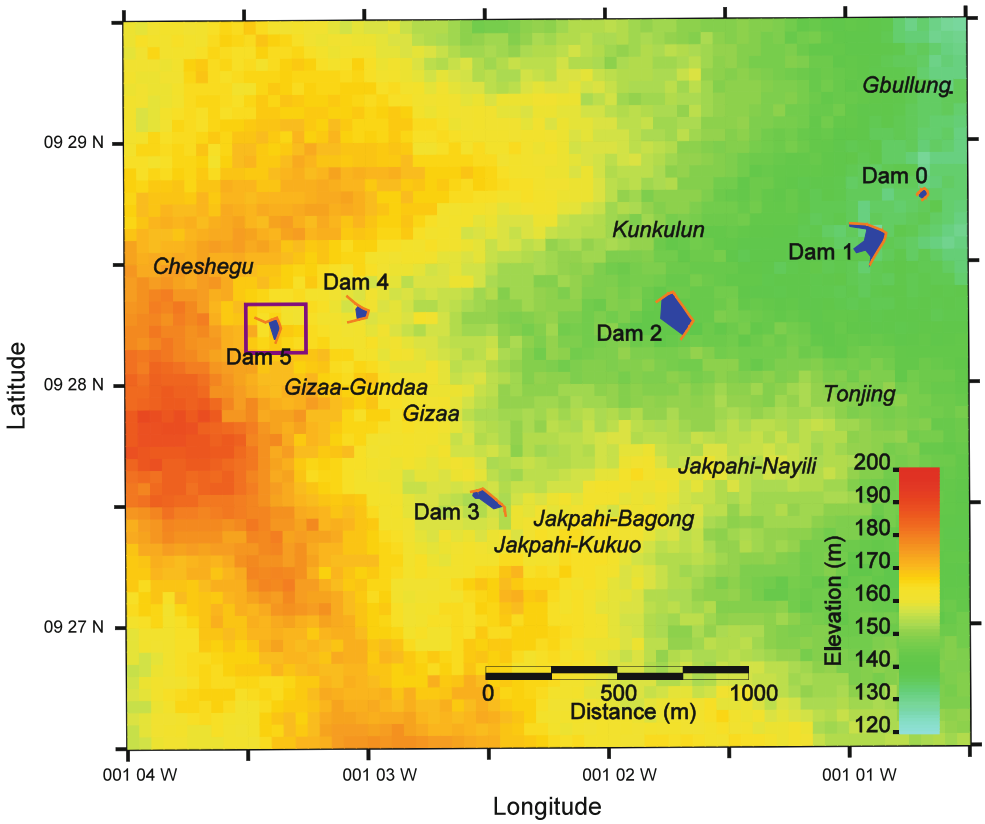

Fig. 1 Six micro-dams in relief of the inland valley and location of the irrigation scheme

Fig. 2 Satellite image of the micro-dam irrigation scheme

the dominant source of water losses in Dam 5. Filling up time of the reservoir during the rainy seasons significantly varies from year to year. The rising trend of the full water level over the years is due to siltation occurring at the upstream side of the reservoir, where the concrete spillway is installed. Here, the full supply water level (FSL) is set as EL168.0m, which is the crest level of the concrete spillway, while the dead-storage level (DSL) is assumed to be EL166.4m. As marked on the time axis of Fig. 3, four dry periods (DP07/08 through DP10/11) during which the water level of Dam 5 monotonically decreases are extracted from the whole observation period. The arithmetic mean (AM) and the standard deviation (SD) of the water level decrease in 24 h are calculated for each dry period and summarized in Table 1 together with its starting date, ending date, and duration.

Using information obtained from water level data, satellite images and field surveys, the water surface area A of Dam 5 is related to the water depth h down to the DSL as

$$A = A(h) = -926.07h^2 + 12510h \tag{1}$$

implying that

$$x = x(h) = -308.69h^3 + 6255.0h^2 \tag{2}$$

where x is the storage volume. The best fit curve for the relation between x and A is

$$A = A(x) = A_{\max}\left(\frac{x}{V}\right)^{0.47} \tag{3}$$

where $A_{\max} = A(h_{\max})$, $V = x(h_{\max})$, and $h_{\max}$ are the water surface area, the storage volume, and the water depth, respectively at FSL. These values are calculated as $A_{\max} = 17{,}645\ \mathrm{m}^2$, $V = 14{,}748\ \mathrm{m}^3$, and $h_{\max} = 1.6$ m, respectively.

There is no evidence that water from Dam 5 has been used for dry season irrigation, which is also not common in the area (Yiridoe et al. 2006). One of the motivations for developing the micro-dam irrigation scheme with Dam 5 is that farmers from a nearby community carried out small-scale gardening using the water from another of the six micro-dams, particularly, Dam 1 located at coordinates 09°28′36″N 001°00′50″W, during the dry season of early 2010. An exceptional torrential rain of 110 mm for one night on February 12th recovered the water levels of the reservoirs and might trigger off the farmers' dry season small-scale gardening. Dam 1 is located 4.8 km downstream from Dam 5 and is rather a simple dugout intended for livestock watering, equipped with an intake pipe to draw water from the reservoir to a cattle trough. The catchment area of Dam 1 is 1,226 ha, including those of Dam 2 through Dam 5. At the time of the small-scale gardening, water was diverted from the cattle trough to basins with beds for the cultivation of *Hibiscus calyphyllus*, which provides vegetable leaves for human

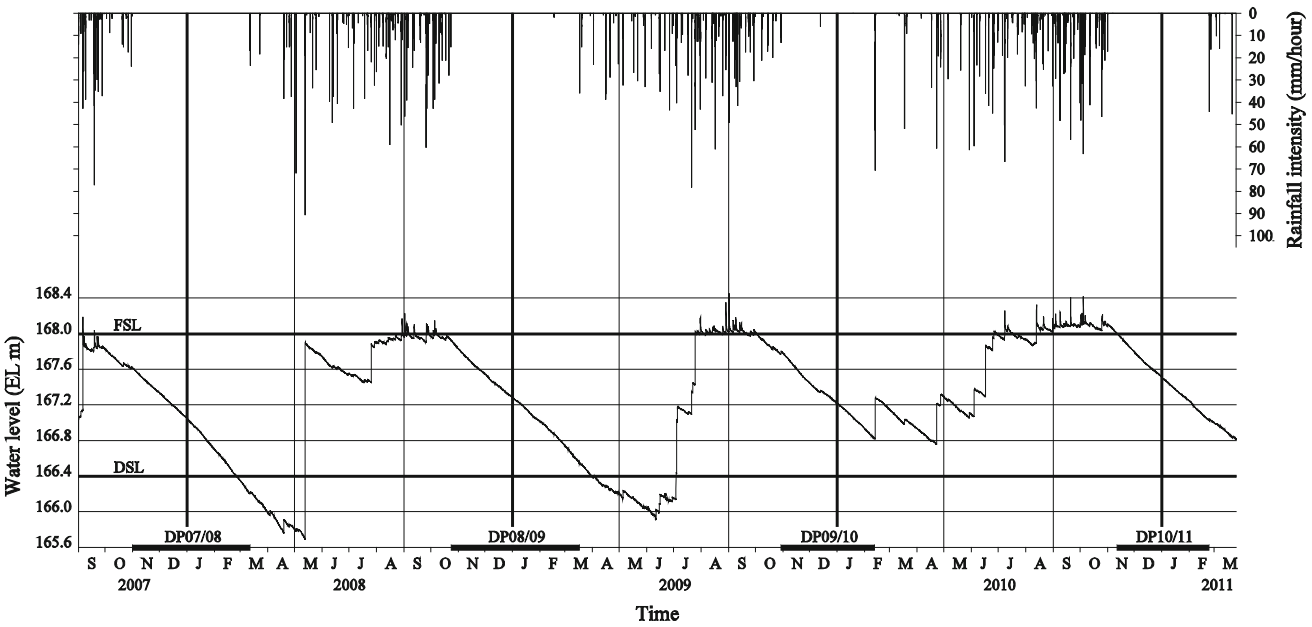

Fig. 3 Observed time series data of rainfall intensity and water level of Dam 5

Table 1 Estimation of water loss during dry periods in Dam 5

Dry period	Starting date	Ending date	Duration (day)	Water level decrease in 24 h	
				AM (mm)	SD (mm)
DP07/08	November 1, 2007	March 11, 2008	132	10.74	3.51
DP08/09	October 24, 2008	March 16, 2009	144	9.51	3.80
DP09/10	October 30, 2009	February 11, 2010	105	9.62	3.14
DP10/11	November 12, 2010	February 22, 2011	103	9.42	3.02

consumption as well as fiber materials. The dimensions of Dam 1 are as large as $h_{\max} = 1.8$ m, $A_{\max} = 91{,}733$ m^2, and $V = 79{,}320$ m^3, while the total area of the command is 350 m^2.

The area immediately downstream side of Dam 5, which is triangular in shape as shown in Fig. 2, is proposed as the potential command area of the micro-dam irrigation scheme. One side of the triangular area is the dam embankment and the other two are planted with trees, so as to control entry of animals. The total area is $a = 840$ m^2, and the land surface slope is less than 1% around an elevation of EL166.35m. Located in the hydromorphic valley bottom, the soil of the area is moderately permeable Dystric Planosols, which is normally used for rice cultivation (CERSGIS 2005). However, rainfed farming system for upland crops such as maize, yam, and groundnut is currently practiced in the area, since Dam 5 bypasses surface water flows which originally covered the valley bottoms during the rainy seasons.

Top soil in the depth between 0.0 and 0.2 m is considered as the target layer for irrigation. In this layer of $D = 0.2$ m thickness, the soil texture is classified as loam (sand 50%, silt 40%, clay 10%). The soil moisture and matric head data were simultaneously collected at a site close to the command area as shown in Fig. 4. Then, the wilting point θ_w, the field capacity θ_c, and the saturation θ_s in terms of volumetric water content are estimated as 0.05, 0.30 at most, and 0.52, respectively. It is assumed that $\theta_{\max}$, the upper limit of tolerable volumetric water content, is equal to 0.35, being a value between θ_c and θ_s. Based on the estimation and the observation by Faulkner et al. (2008), a reasonably large value of 20 mm/day is assumed for E_c, the average water consumption rate. However, there are different small-holder farmers' practices to conserve soil moisture in the semi-arid SSA (Chiroma et al. 2006), making it difficult to determine the actual water consumption rate, which may include evapotranspiration varying with different growth stages, deep percolation, conveyance losses, and so on. The volumetric water content θ that can be observed may differ from the actual one. The model proposed here comprehensively represents these uncertainties in terms of the stochastic processes, where

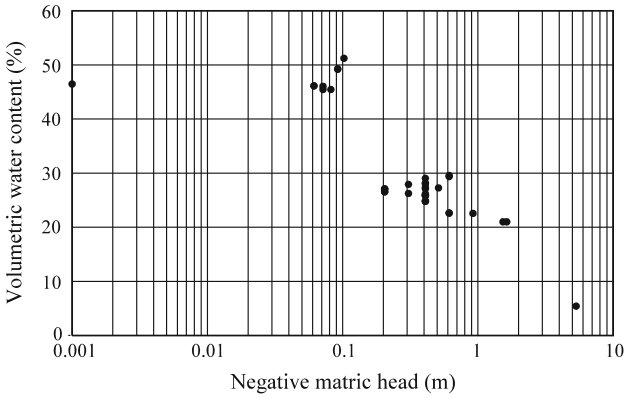

Fig. 4 Soil moisture and matric head data collected at the site of a hydromorphic valley bottom

volatility is the sole model parameter prescribing the magnitude of fluctuations.

Dam 5 is not equipped with water intake facilities available for the command area. Using solar photovoltaic (PV) powered electric pumps is a feasible option for lifting water from the reservoir, since solar PV electrification is developing in the rural areas of Ghana (Obeng and Evers 2010). A PV pumping system unit consisting of a submerged electric direct current (DC) pump and a solar panel without a rechargeable battery is commercially available, and it can operate during daylight hours from 09:00 to 15:00 with the expected solar radiation at the site. Every PV pumping system unit is assumed to be equipped with a 12 mm diameter hose with a Manning's roughness coefficient of 0.01, crossing over the dam embankment, in order to convey the irrigation water from the DSL of the reservoir to the command area. Then, the operating flow rate Q_P (L/min) of a single PV pumping system unit is related to the storage volume x as

$$Q_P = Q_P(x) = 8.680 + 1.243\left(\frac{x}{V}\right)^{0.53}. \tag{4}$$

3 Stochastic model and optimal control

The dynamics of the micro-dam irrigation scheme is modeled as a system of two stochastic differential equations

$$\begin{cases} \mathrm{d}X_t = (Q(X_t) - u)\mathrm{d}t \\ \mathrm{d}Y_t = (u - \bar{q}(Y_t))\mathrm{d}t + \sigma(Y_t)\mathrm{d}B \end{cases} \tag{5}$$

where X_t is the storage volume of the reservoir at the time t, Y_t is the volume of readily available water contained in the soil of the command area at the time t, Q is the uncontrolled water balance flowing into the reservoir, u is the intake flow rate from the reservoir for irrigation in the command area, $\bar{q}$ is the average volumetric water consumption rate in the command area, σ is the volatility of soil moisture in the command area, and B is the one-dimensional Brownian motion. The presence of the stochastic term $\sigma(Y_t)\mathrm{d}B$ involves including all uncertainties. The farmers that manage the micro-dam irrigation scheme are assumed to know the current states of X_t and Y_t so as to give feed-back to u. A temporal domain $(0, T)$ is considered as the maximum irrigation period, whose duration is equal to T. The worst case considered is the drying up of either the reservoir or the command area during the course of the irrigation period, bringing the irrigation scheme to ruin. Reaching $\theta_{\max}$ of the volumetric water content is not tolerated. Exceeding $h_{\max}$ of the water depth of the reservoir is unfavorable, though it does not happen almost surely. Thus, a spatial x–y domain of the stochastic processes (X_t, Y_t) is prescribed as

$$\Omega_x \times \Omega_y = (0,\ V) \times (y_{\min}, y_{\max}) \tag{6}$$

where $y_{\min} = aD\theta_w$, and $y_{\max} = aD\theta_{\max}$. Then, the stochastic control problem is mathematically formulated as maximization of the cost function

$$J^u(s,x,y) = E^{s,x,y}\left[g\left(\hat{T}, X_{\hat{T}}, Y_{\hat{T}}\right)\right] \tag{7}$$

where $\hat{T}$ is the first exit time of (X_t, Y_t) from the spatio-temporal domain $(0, T) \times \Omega_x \times \Omega_y$, and g is the function evaluating the severity of the ruin. Setting

$$g\left(\hat{T}, X_{\hat{T}}, Y_{\hat{T}}\right) = g\left(\hat{T}\right) = -\frac{T - \hat{T}}{T} \tag{8}$$

is appropriate in the sense that it is continuous on the boundary of $(0, T) \times \Omega_x \times \Omega_y$, monotone increasing with respect to $\hat{T}$, and vanishing at $\hat{T} = T$. The intake flow rate u is constrained in the set U of admissible controls, which is the closed interval $[u_{\min}, u_{\max}]$. An optimal control u^* is $u = u(s, x, y)$ that achieves the maximum of the cost function $J^u(s, x, y)$, satisfying $u_{\min} \le u \le u_{\max}$. The expectation of the first exit time $\hat{T}^*$ under the optimal control u^* is inversely given by

$$E^{s,x,y}\left[\hat{T}^*\right] = T\left(1 - J^{u^*}(s,x,y)\right). \tag{9}$$

According to Øksendal (2007), the maximum Φ of $J^u(s, x, y)$ and the optimal control u^* are governed by the HJB equation

$$\frac{\partial\Phi}{\partial s} + (Q - u^*)\frac{\partial\Phi}{\partial x} + (u^* - \bar{q})\frac{\partial\Phi}{\partial y} + \frac{\sigma^2}{2}\frac{\partial^2\Phi}{\partial y^2} = 0 \tag{10}$$

with the boundary condition

$$\Phi(s,x,y) = g(s,x,y). \tag{11}$$

The HJB equation (Eq. 10) is rewritten as

$$\frac{\partial\Phi}{\partial s} + Q(x)\frac{\partial\Phi}{\partial x} - \bar{q}\frac{\partial\Phi}{\partial y} + \frac{\sigma^2}{2}\frac{\partial^2\Phi}{\partial y^2} - zu^* = 0 \tag{12}$$

where z is the multiplier

$$z = \frac{\partial \Phi}{\partial x} - \frac{\partial \Phi}{\partial y} \tag{13}$$

from which the optimal control u^* is determined as

$$u^* = \begin{cases} u_{\max} & (z<0) \\ \text{any} & (z=0) \\ u_{\min} & (z>0) \end{cases} \tag{14}$$

so as to maximize the left hand side of (Eq. 10).

4 Computational method and application

As a consequence of the discussions in the preceding sections, the model parameters are determined as summarized in Table 2, where y_s is the volume of water contained in the soil of the command area when saturated. However, the volatility σ is assumed to be a positive convex function in Ω_y with a constant parameter C_v in the form

$$\sigma = \sigma(y) = C_v \frac{y_s - y}{y_s - y_{\min}} y, \tag{15}$$

so that σ vanishes when the soil moisture is at the wilting point or when the soil is saturated. In designing a control system, specifying the value of C_v implies how much fluctuation is presumed in the soil moisture.

The bounds of the set of admissible controls become

$$u_{\min} = 0 \tag{16}$$

and

$$u_{\max} = u_{\max}(s,x) = \begin{cases} N_P Q_P(x) & (9 < \mathrm{mod}(24s, 24) < 15) \\ 0 & (\text{Otherwise}) \end{cases} \tag{17}$$

where N_P is the number of the PV pumping system units. Here, N_P is chosen as eight (8), so that averaged $u_{\max}$ cover $\bar{q}$.

The finite element method is employed for numerically solving the partial differential equation Eq. 10 to obtain Φ and u^* as functions of s, x, and y. The same upwind discretization scheme as in Unami et al. (2010) is applied to the weak form of Eq. 10, which is written as

$$\int_{\Omega_y} \left(w \frac{\partial \Phi}{\partial s} + w(Q - u^*) \frac{\partial \Phi}{\partial x} + w(u^* - \bar{q}) \frac{\partial \Phi}{\partial y} - \frac{1}{2} \frac{\partial (w\sigma^2)}{\partial y} \frac{\partial \Phi}{\partial y} \right) \mathrm{d}y = 0 \tag{18}$$

for any weight w in $H_0^1(\Omega_y)$, the space of functions having certain regularity properties in Ω_y and vanishing at the boundary of Ω_y. The spatial domain $\Omega_x \times \Omega_y$ is discretized into rectangular sub-domains of equal size Δx by Δy, which are generically represented as $(i\Delta x, (i+1)\Delta x) \times (k\Delta y, (k+1)\Delta y)$ for integers i and k. The unknown Φ is attributed to each node $(i\Delta x, k\Delta y)$ and is denoted by $\Phi_{i,k}$. Then, there are four estimates $z_{\pm\pm}$ for the multiplier z in each subdomain;

$$z_{--} = \frac{\Phi_{i+1,k} - \Phi_{i,k}}{\Delta x} - \frac{\Phi_{i,k+1} - \Phi_{i,k}}{\Delta y}, \tag{19}$$

$$z_{-+} = \frac{\Phi_{i+1,k+1} - \Phi_{i,k+1}}{\Delta x} - \frac{\Phi_{i,k+1} - \Phi_{i,k}}{\Delta y}, \tag{20}$$

$$z_{+-} = \frac{\Phi_{i+1,k} - \Phi_{i,k}}{\Delta x} - \frac{\Phi_{i+1,k+1} - \Phi_{i+1,k}}{\Delta y}, \tag{21}$$

and

$$z_{++} = \frac{\Phi_{i+1,k+1} - \Phi_{i,k+1}}{\Delta x} - \frac{\Phi_{i+1,k+1} - \Phi_{i+1,k}}{\Delta y}. \tag{22}$$

As a computational rule applied to each sub-domain, the rigor of Eq. 14 is relaxed as

$$u^* = \frac{\mu}{4} u_{\max} \tag{23}$$

where μ is the number of negative estimates $z_{\pm\pm}$. Practically, the number n_P of operating pumps may be 0, 2, 4, 6, or 8. Finally, imposing the boundary condition Eq. 11 and employing a fully implicit scheme in the temporally backward direction with an increment Δs, a system of linear equations is composed for updating the values of $\Phi_{i,k}$ and is solved with the Gauss–Seidel method. However, a predictor–corrector scheme is further applied so that the optimal control is determined not with the future values of $\Phi_{i,k}$ but with the current ones.

Specifying three different values of C_v as 0.20, 0.30, and 0.40, the computational procedure is implemented. The computational grid sizes are $\Delta x = \frac{V}{150}$, $\Delta y = \frac{y_{\max} - y_{\min}}{150}$, and $\Delta s = \frac{1}{1{,}440}$ day (1 min). The results at noon are shown in Figs. 5, 6 and 7 in terms of n_P under the optimal water management strategy and $E^{s,x,y}\left[\hat{T}^*\right]$, with halving temporal intervals (68, 34, and 17 days) so that both the first and the last days are included. The diagrams of n_P on the x–y plane outline the irrigation principle, which is based on supply-side strategy when $\left|\frac{\partial n_P}{\partial x}\right| \gg \left|\frac{\partial n_P}{\partial y}\right|$ and demand-side strategy when $\left|\frac{\partial n_P}{\partial x}\right| \ll \left|\frac{\partial n_P}{\partial y}\right|$. Stopping all the pumps when the reservoir is near empty is an obvious supply-side strategy, as

Table 2 Key parameters used for the optimal control of the micro-dam irrigation scheme

T	V	$y_{\min} = aD\theta_w$	$y_{\max} = aD\theta_{\max}$	$y_s = aD\theta_s$	$\bar{q} = aE_c$
120 days	14,748 m^3	8.40 m^3	58.80 m^3	87.36 m^3	16.80 m^3/day

is computationally reproduced, but otherwise demand-side strategy is predominant in all cases of C_v-values. Switching θ, which is defined as the maximum volumetric water content where all the pumps should operate, varies with s and x when $C_v = 0.20$ but is almost constant at 20–25% when $C_v = 0.30$ and 0.40. Gray zones with $n_P = 2$, 4, or 6 appear where the expected first exit time is almost constant in the x–y plane, as Eq. 13 indicates. Minor numerical oscillations in appearance of the gray zones are seen when the reservoir is near full.

The numerical solutions of Φ are totally oscillation free. The contour graphs of $E^{s,x,y}\left[\hat{T}^*\right]$ on the x–y plane quantitatively represent the performance of the optimal water management strategy. The minimum of $E^{s,x,y}\left[\hat{T}^*\right]$ is achieved on the boundary of $\Omega_x \times \Omega_y$ for every s. The subdomain of $\Omega_x \times \Omega_y$ where the value of $E^{s,x,y}\left[\hat{T}^*\right]$ is large appears near the boundary $x = V$ with moderate y, and then it expands to the whole $\Omega_x \times \Omega_y$ as the time s approaches to T. A critical time s_c, which is defined as the minimum

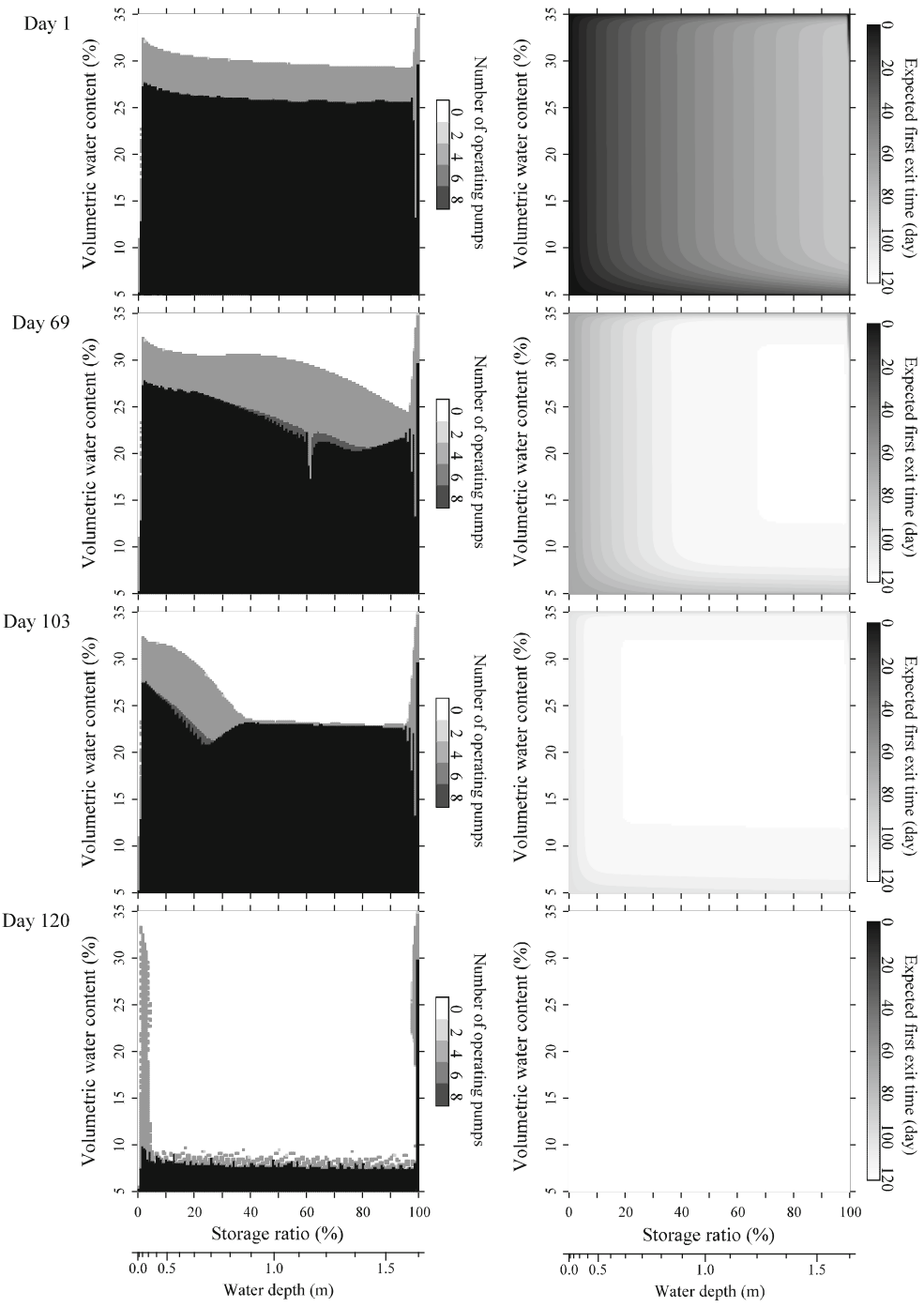

Fig. 5 Number of operating pumps (*left column*) and expected first exit time (*right column*) for $s = 12{:}00$ h of the 1st, the 69th, the 103th, and the 120th days with $C_v = 0.20$

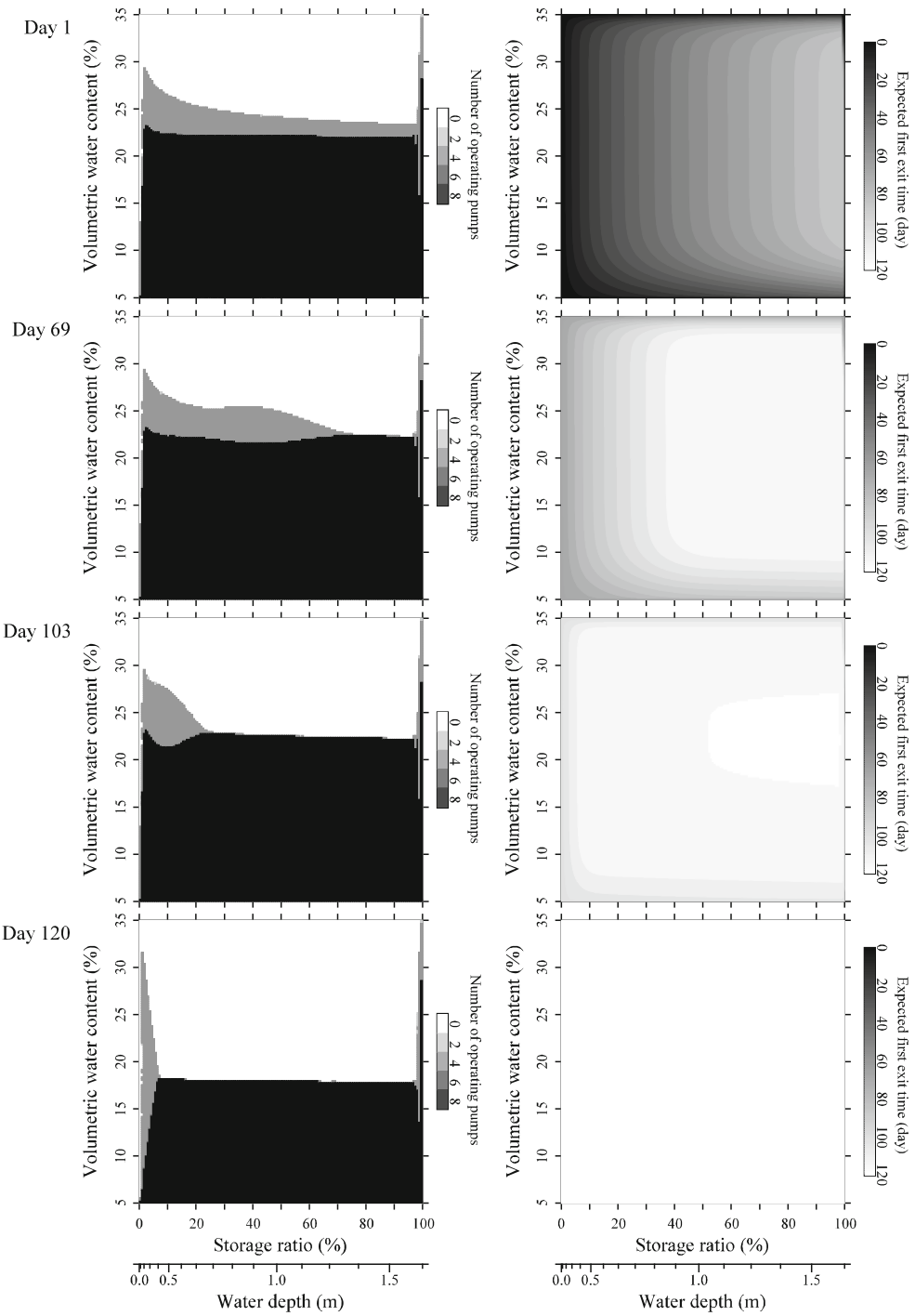

Fig. 6 Number of operating pumps (*left column*) and expected first exit time (*right column*) for $s = 12{:}00$ h of the 1st, the 69th, the 103th, and the 120th days with $C_v = 0.30$

s where there exists (x, y) such that the expected first exit time $E^{s,x,y}\left[\hat{T}^*\right]$ is greater than 119 days, is on the 38th, 39th, and 96th day for $C_v = 0.20$, 0.30, and 0.40, respectively. In other words, the micro-dam irrigation scheme can be expected to last for about 80 days if $C_v = 0.20$ or 0.30, provided that the reservoir is full and the soil moisture of the command area is moderate at the initial stage. While, the micro-dam irrigation scheme becomes short of water within 24 days if the value of C_v is larger as 0.40.

For the sake of comparison, another computational run for $C_v = 0.20$, the least severe case, is implemented with $u^* = u_{\max}$, implying that the pumps are always operated at full capacity. The results are shown in Fig. 8. The critical time s_c is on the 116th day. Unlike the controlled cases, the value of $E^{s,x,y}\left[\hat{T}^*\right]$ is almost uniform in the whole $\Omega_x \times \Omega_y$ at every stage of time.

The computational procedure is implemented for different values of the command area a as well, though

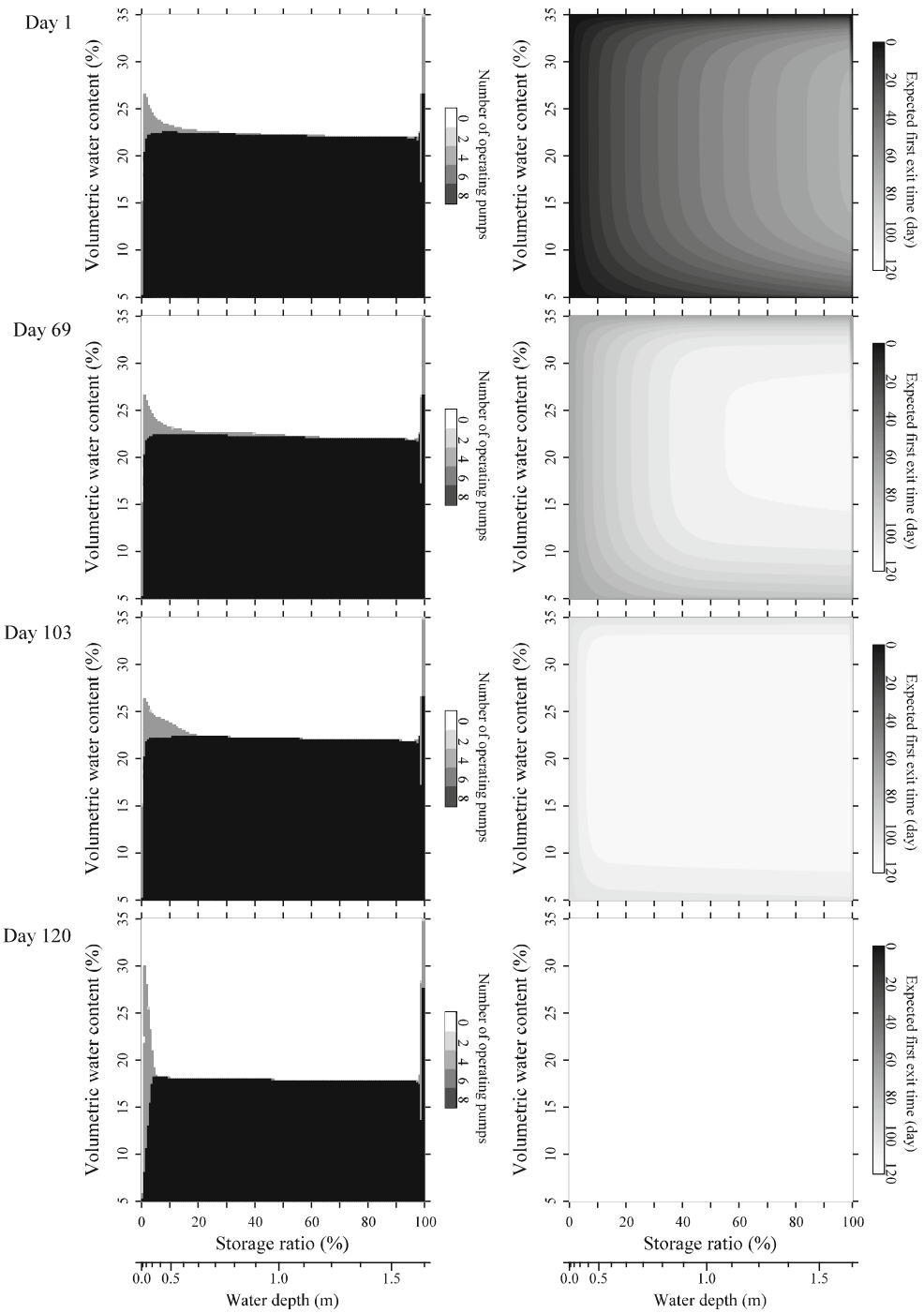

Fig. 7 Number of operating pumps (*left column*) and expected first exit time (*right column*) for $s = 12{:}00$ h of the 1st, the 69th, the 103th, and the 120th days with $C_v = 0.40$

detailed results are not presented here. When $a = 420$ m^2, half of the original value, the critical time s_c is on the 33th, 34th, and 90th day for $C_v = 0.20$, 0.30, and 0.40, respectively. When $a = 210$ m^2, one quarter of the original value, the critical time s_c is on the 31th, 32th, and 90th day for $C_v = 0.20$, 0.30, and 0.40, respectively. Qualitative behavior of the numerical solutions of u^* and Φ for these values of a is almost the same as that for the original $a = 840$ m^2, except that switching θ shifts to the dry side and the gray zones increase as the value of a becomes small. In practice, soil moisture should be controlled on the dry side if the command area is small, but it has the least effect of prolonging the irrigation period. When $a = 1{,}680$ m^2, the double of the original value, the critical time s_c is on the 110th, 112th, and 115th day for $C_v = 0.20$, 0.30, and 0.40, respectively. In that case there is

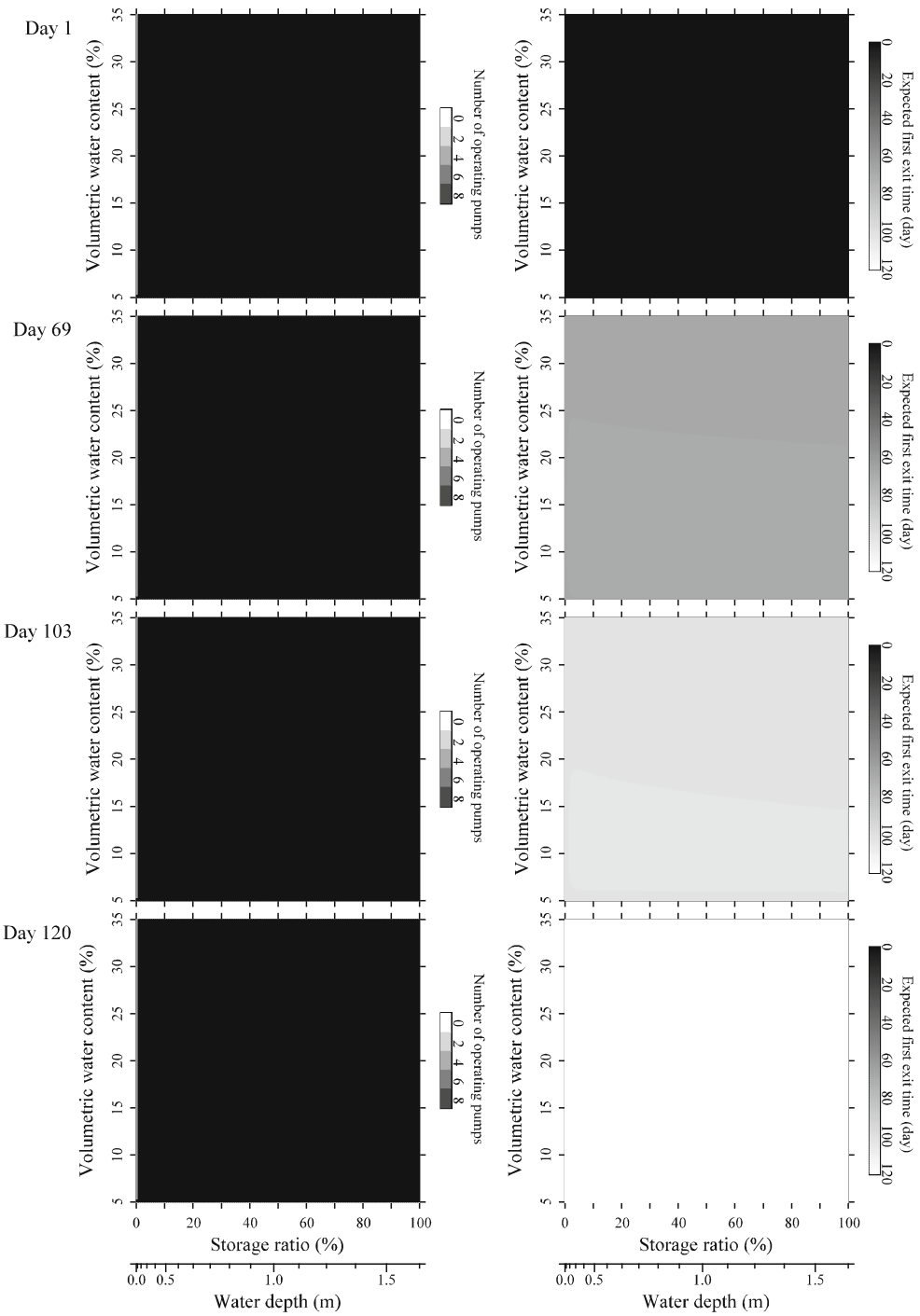

Fig. 8 Number of operating pumps (*left column*) and expected first exit time (*right column*) for $s = 12{:}00$ h of the 1st, the 69th, the 103th, and the 120th days with $C_v = 0.20$, not using the optimal control

substantially no possibility of successful dry season farming in the enlarged micro-dam irrigation scheme.

The results obtained above indicate that the rigorous stochastic control approach with the minimum model leads to simple optimal management strategies, which is consistent with common conventional practices of small-scale subsistence farming. This methodology is advantageous over the conventional scenario-based optimization by not requiring many ambiguous model parameters as well as offering feasible solutions at the community level.

5 Conclusions

A stochastic control approach is applied to the optimal water management of an irrigation scheme consisting of a reservoir, a command area, and water intake facilities. Only the first exit time is considered as the performance index, targeting at small-scale subsistence farming where profit is not a primary concern. The computational procedure that solves the HJB equation for the stochastic processes provides comprehensive information on the optimal

control. Demonstrations are given for the micro-dam irrigation scheme planned at a site within the Guinea savanna agro-ecological zone of West Africa. The model parameters are estimated by different observed data, with specified values of volatility. No inflow is expected into the reservoir and the evapotranspiration is extremely high during the dry seasons, when the irrigation scheme is operational. This is a very severe condition observed here, which is not encountered in neither the Monsoon Asia nor in East Africa. Though the capacity of the micro-dam is seemingly large relative to the small command area, the computational results indicated that the irrigation scheme cannot last long enough for the cultivation of dry season crops when the volatility is too large. When the volatility is small enough, the initial water stored in the reservoir can support full irrigation for about 80 days under the optimal water management strategy, which is predominantly based on the demand-side principle. The feed-back rule is so simple that water should be taken from the reservoir when the command area requires water, and it is considered feasible at the community level. These facts explain the actual farmers' practice of small-scale gardening in the smaller command area using the water from the larger reservoir. However, introduction of water intake facilities such as the PV pumping system unit will be a constraint to realizing the potential of the irrigation scheme.

Acknowledgments This research was funded by a grant-in-aid for scientific research No. 20255012, from the Japan Society for the Promotion of Science. The authors also thank Mr. F. K. Abagale, University for Development Studies, Ghana, as well as the communities in Tolon/Kumbungu District of Northern Region, Ghana, for their valuable support in the field studies.

References

Arumugam N, Mohan S (1997) Integrated decision support system for tank irrigation system operation. J Water Resour Plan Manage 123(5):266–273

Baten MA, Miah ABMAS (2007) Optimal consumption in a growth model with the CES production function. Stoch Anal Appl 25(5):1025–1042

Carter R, Kay M, Weatherhead K (1999) Water losses in smallholder irrigation schemes. Agric Water Manage 40(1):15–24

Centre for Remote Sensing and Geographic Information Service (CERSGIS) (2005) FAO soil classification map for SLaM study site in Fihini area. University of Ghana, Legon

Chaumont S, Imkeller P, Müller M (2006) Equilibrium trading of climate and weather risk and numerical simulation in a Markovian framework. Stoch Env Res Risk Assess 20(3): 184–205

Chiroma AM, Folorunso OA, Alhassan AB (2006) Soil water conservation, growth, yield and water use efficiency of sorghum as affected by land configuration and wood-shavings mulch in semi-arid northeast Nigeria. Exp Agric 42(2):199–216

Farr TG, Rosen PA, Caro E, Crippen R, Duren R, Hensley S, Kobrick M, Paller M, Rodriguez E, Roth L, Seal D, Shaffer S, Shimada J, Umland J, Werner M, Oskin M, Burbank D, Alsdorf D (2007) The shuttle radar topography mission. Rev Geophys 45:RG2004

Faulkner JW, Steenhuis T, van de Giesen N, Andreini M, Liebe JR (2008) Water use and productivity of two small reservoir irrigation schemes in Ghana's Upper East region. Irrigation Drainage 57(2):151–163

Guerra LC, Watson PG, Bhuiyan SI (1990) Hydrological analysis of farm reservoirs in rainfed rice areas. Agric Water Manage 17(4):351–366

International Institute for Land Reclamation and Improvement (ILRI) (1993) Inland valleys in West Africa: an agro-ecological characterization of rice-growing environments. In: Windmeijer PN, Andriesse W (ed), ILRI Publication 52, pp 37–44

Kulecho IK, Weatherhead EK (2005) Reasons for smallholder farmers discontinuing with low-cost micro-irrigation: a case study from Kenya. Irrigation Drainage Syst 19(2):179–188

Leemhuis C, Jung G, Kasei R, Liebe J (2009) The Volta Basin water allocation system: assessing the impact of small-scale reservoir development on the water resources of the Volta basin, West Africa. Adv Geosci 21:57–62

Liebe J, van de Giesen N, Andreini MS (2005) Estimation of small reservoir capacities in semi-arid environment. A case study in the Upper East Region of Ghana. Phys Chem Earth 6(7): 448–454

Liebe J, van de Giesen N, Andreini MS, Steenhuis TS, Walter MT (2009) Suitability and limitations of ENVISAT ASAR for monitoring small reservoirs in a semiarid area. IEEE Transac Geosci Remote Sens 47(5):1536–1547

Lu HW, Huang GH, He L (2009) An inexact programming method for agricultural irrigation systems under parameter uncertainty. Stoch Env Res Risk Assess 23(6):759–768

Makurira H, Mul ML, Vyagusa NF, Uhlenbrook S, Savenije HHG (2007) Evaluation of community-driven smallholder irrigation in dryland South Pare Mountains, Tanzania: a case study of Manoo micro dam. Phys Chem Earth 32(15–18):1090–1097

Mdemu MV, Rodgers C, Vlek PLG, Borgadi JJ (2009) Water productivity (WP) in reservoir irrigated schemes in the upper east region (UER) of Ghana. Phys Chem Earth 34:324–328

Morimoto H, Kawaguchi K (2002) Optimal exploitation of renewable resources by the viscosity solution method. Stoch Anal Appl 20(5):927–946

Mul ML, Kemerink JS, Vyagusa NF, Mshana MG, van der Zaag P, Makurira H (2011) Water allocation practices among smallholder farmers in the South Pare Mountains, Tanzania: the issue of scale. Agric Water Manage 98(11):1752–1760

Ngigi SN, Savenije HHG, Thome JN, Rockström J, de Vries FWTP (2005) Agro-hydrological evaluation of on-farm rainwater storage systems for supplemental irrigation in Laikipia district Kenya. Agric Water Manage 73(1):21–41

Obeng GY, Evers HD (2010) Impacts of public solar PV electrification on rural micro-enterprises: the case of Ghana. Energy Sustain Dev 14(3):223–231

Øksendal B (2007) Stochastic differential equations. Springer-Verlag, Berlin 6th edn, corrected 4th printing, pp 237–261

Pachpute JS, Tumbo SD, Sally H, Mul ML (2009) Sustainability of rainwater harvesting systems in rural catchment of Sub-Saharan Africa. Water Resour Manag 23(13):2815–2839

Panigrahi B, Panda SN, Mal BC (2007) Rainwater conservation and recycling by optimal size on-farm reservoir. Resour Conserv Recycl 50(4):459–474

Senzanje A, Boelee E, Rusere S (2008) Multiple use of water and water productivity of communal small dams in the Limpopo Basin, Zimbabwe. Irrigation Drainage Syst 22:225–237

Srivastava RC (1996) Design of runoff recycling irrigation system for rice cultivation. J Irrigation Drainage Eng 122(6):331–335

Srivastava RC, Kannan K, Mohanty S, Nanda P, Sahoo N, Mohanty RK, Das M (2009) Rainwater management for smallholder irrigation and its impact on crop yields in eastern India. Water Resour Manag 23(7):1237–1255

Unami K, Alam AHMB (in press) Concurrent use of finite element and finite volume methods for shallow water flows in locally 1-D channel networks. Int J Num Methods Fluids

Unami K, Kawachi T, Yangyuoru M (2005) Optimal water management in small-scale tank irrigation systems. Energy 30: 1419–1428

Unami K, Kawachi T, Kranjac-Berisavljevic G, Abagale FK, Maeda S, Takeuchi J (2009) Case study: hydraulic modeling of runoff processes in Ghanaian inland valleys. J Hydraulic Eng 135(7): 539–553

Unami K, Abagale FK, Yangyuoru M, Alam AHMB, Kranjac-Berisavljevic G (2010) A stochastic differential equation model for assessing drought and flood risks. Stoch Env Res Risk Assess 24(5):725–733

Unami K, Yangyuoru M, Alam AHMB (2012) Rationalization of building micro-dams equipped with fish passages in west African savannas. Stoch Env Res Risk Assess 26(1):115–126

Yiridoe EK, Langyintuo AS, Dogbe W (2006) Economics of the impact of alternative rice cropping systems on subsistence farming: whole-farm analysis in northern Ghana. Agric Syst 91:102–121

Yiu KFC, Liu J, Siu TK, Ching WK (2010) Optimal portfolios with regime switching and value-at-risk constraint. Automatica 46(6): 979–989